

# Structure and Electron Density of (2,2,2-Trifluoro-1-methylethylidene)sulfur Tetrafluoride, $F_4S=C(CH_3)CF_3$

J. Buschmann,<sup>†</sup> T. Koritsanszky,<sup>‡</sup> R. Kuschel,<sup>§</sup> P. Luger,<sup>†</sup> and K. Seppelt<sup>\*§</sup>

Contribution from the Institut für Anorganische und Analytische Chemie and the Institut für Kristallographie, Freie Universität, D-1000 Berlin, West Germany, and the Central Research Institute for Chemistry of the Hungarian Academy of Sciences, H-1025 Budapest, Hungary.  
Received June 6, 1990

**Abstract:** High-resolution X-ray data were collected at low temperature (-151 (1) °C) to determine the crystal and molecular structure and the electron deformation density (EDD) of  $F_4S=C(CH_3)CF_3$ . Crystal data is as follows:  $a = 1709.0$  (7),  $b = 647.8$  (6),  $c = 1698.0$  (7) pm,  $\beta = 136.96$  (6)°,  $P2_1/n$ ,  $Z = 8$ . The sulfur, the two axial fluorine, and the carbon atoms exhibit a planar arrangement. The equatorial S-F bond distances are significantly shorter than the axial ones. Atomic valence deformations were analyzed in terms of static (SDD) and dynamic deformation densities (DDD) calculated from the fitted multipole populations and X-X Fourier synthesis. The EDD along the S-C bond does not show cylindrical symmetry, i.e., the contours of constant electron density perpendicular to the bond reach out twice as far in the equatorial than in the axial direction. This feature can clearly be attributed to a double bond character. The axial S-F bond appears to be more polarized than the equatorial one. The charge loss at the sulfur atom is shared by the alkylidene and fluorine ligands in a ratio of about 1:2, leading to a polarized S-C bond. In the interpretation of the EDD along the bonds to the F atoms, the proper orientation of the reference density is shown to be useful. To emphasize these bond peaks, the electron density of the promolecule generated with the oriented atom model (OAM) proved itself to be superior to that of the promolecule calculated from spherical atoms.

## Introduction

Phosphorus and sulfur ylides, known since 1919<sup>1</sup> and 1930,<sup>2</sup> have been thoroughly investigated in terms of their structure, bonding, and reactivity.<sup>3-6</sup> In numerous investigations it was found that the ylidic bond in compounds like  $R_3P^+C^-R_2$ ,  $R_2S^+C^-R_2$ , and  $R_2OS^+C^-R_2$  is (a) somewhat shorter than a normal single bond, (b) has a certain polar character that is important with respect to reactivity, and (c) allows free rotation of the two molecular parts connected by this bond.<sup>7</sup> These bonding characteristics are usually described by the ylidic (zwitterionic) formulation. The bonding in the alkylidenesulfur tetrafluorides seems to be different. The C-S bond length of about 155-160 pm<sup>8,9</sup> is significantly shorter than that found in sulfur ylides (171-174 pm)<sup>10-13</sup> and can be regarded as that of a double bond. There seems to be less polarity in the bond, since all alkylidenesulfur tetrafluorides are gases or low boiling liquids and, most important, the C-S bond does not show free torsion up to +100 °C. Furthermore, it has been established that alkylidenesulfur tetrafluorides have a very special geometry. Carbon substituents and the axial fluorine atoms lie in a common plane.<sup>8,14</sup> This was found in the species  $F_4S=CH_2$  and  $F_4S=CHCOF$ , but the question of exact planarity remained in doubt because of the uncertain positions of the hydrogen atoms. The task of this work was to prove the planarity of the  $F_2S=CR_2$  molecular fragment beyond doubt, as these species are possible candidates for "nonclassical distortions" of the double bond.<sup>15</sup> Another important intention was to map the electron deformation density of these novel bond systems, in particular with respect to the C=S double bond. For this reason the measurement of the X-ray reflections was carried out at the low temperature of -151 °C.

The choice of the best suited alkylidenesulfur tetrafluoride from the few known ones,  $F_4S=CH_2$ ,<sup>16</sup>  $F_4S=CHCH_3$ ,<sup>17</sup>  $F_4S=CHCF_3$ ,<sup>18</sup>  $F_4S=CHCOF$ ,<sup>9</sup> and  $F_4S=C(CH_3)CF_3$ ,<sup>18</sup> was easy, since only the last one carries two non-hydrogen ligands on the double-bonded carbon atom. Moreover, for the X-ray structure analysis it was desirable to have a crystal space group of low symmetry in order to avoid crystallographic planarity being forced upon the molecule. These requirements were met with the present structure.

## Experimental Section

**Spectra:** infrared spectra, Perkin Elmer 8983; Raman, Cary 82, Ar laser excitation; mass spectra, Varian 711, 80 eV, EI; and NMR spectra, Jeol FX 90 Q.

**Reagents.**  $F_3SCBr(CH_3)CF_3$  was prepared according to methods given in the literature.<sup>18</sup>  $F_3S=C(CH_3)CF_3$ . For the planned structural investigation special care was taken to obtain pure material. A solution of 24 g (80 mmol) of  $F_3SCBr(CH_3)CF_3$  in 200 mL of anhydrous methylcyclohexane is cooled to -110 °C. Eighty milliliters of  $n-C_4H_9Li$  in 80 mL of  $n-C_6H_{14}$  is added slowly, keeping the temperature below -100 °C. A colorless slurry is formed that dissolves upon slow warming to room temperature. All volatile products are pumped in vacuo into a cold trap of -196 °C until only methylcyclohexane remains. The condensate is distilled in a spinning band column, until the boiling point of  $n-C_6H_{14}$  (69 °C) is reached. Preparative gas chromatography on a 2-m long, 1-cm wide glass column, chromosorb PAW 80/100 mesh, 15% squalane, yields 5.6 g (27%) of pure  $F_4S=C(CH_3)CF_3$  as a colorless, stable liquid: bp

- (1) Staudinger, H.; Meyer, J. *Helv. Chim. Acta* **1919**, *2*, 639.
- (2) Ingold, C. K.; Jessup, J. A. *J. Chem. Soc. (London)* **1930**, 713.
- (3) Schmidbaur, H. *Acc. Chem. Res.* **1975**, *8*, 62.
- (4) Bestmann, H. *J. Pure Appl. Chem.* **1980**, *52*, 771.
- (5) Claus, P. K. In *Houben Weyl*, Klamann, D., Ed.; G. Thieme Verlag Stuttgart: New York, 1985; Vol. E11, p 1344.
- (6) Frost, B. U.; Malvin, L. S., Jr. *Sulfur Ylides*; Academic Press: New York, 1975; Vol. 31, Organic chemistry.
- (7) Only in  $FCOCH=SF_2O$  does the increased double bond character of the C-S bond give rise to two isomers below -40 °C, which is probably caused by the fluorine substitution on sulfur: Krügerke, T.; Seppelt, K. *Chem. Ber.* **1988**, *121*, 1977.
- (8) Simon, A.; Peters, E. M.; Lentz, D.; Seppelt, K. *Z. Anorg. Allg. Chem.* **1980**, *468*, 7.
- (9) Krügerke, T.; Buschmann, J.; Kleemann, G.; Luger, P.; Seppelt, K. *Angew. Chem.* **1987**, *99*, 808; *Angew. Chem., Int. Ed. Engl.* **1987**, *26*, 799.
- (10) Christensen, A. T.; Witmore, W. G. *Acta Crystallogr., Sect. B.* **1969**, *25*, 73.
- (11) Adrianov, G.; Struchkov, Y. T. *Izv. Akad. Nauk SSSR* **1977**, *26*, 687; *Bull. Acad. Sci. USSR, Div. Chem. Sci. (Engl. Trans.)* **1977**, *26*, 634.
- (12) Christensen, A. T.; Thom, E. *Acta Crystallogr., Sect. B.* **1971**, *27*, 581.
- (13) Atwood, J. L.; Mayfield, H. T. *Cryst. Struct. Commun.* **1978**, *7*, 739.
- (14) Krügerke, T.; Buschmann, J.; Kleemann, G.; Luger, P.; Seppelt, K. *Angew. Chem.* **1987**, *99*, 808; *Angew. Chem., Int. Ed. Engl.* **1987**, *26*, 799.
- (15) Trinquier, G.; Malrieu, J.-P. *J. Am. Chem. Soc.* **1987**, *109*, 5303.
- (16) Kleemann, G.; Seppelt, K. *Angew. Chem.* **1978**, *90*, 5471; *Angew. Chem. Int. Ed. Engl.* **1978**, *17*, 516; *Chem. Ber.* **1983**, *116*, 645.
- (17) Pötter, B.; Seppelt, K. *Inorg. Chem.* **1982**, *21*, 3147.
- (18) Pötter, B.; Kleemann, J.; Seppelt, K. *Chem. Ber.* **1984**, *120*, 3255.

<sup>†</sup> Institut für Kristallographie, FU Berlin.

<sup>‡</sup> Central Research Institute for Chemistry of the Hungarian Academy of Sciences.

<sup>§</sup> Institut für Anorganische und Analytische Chemie, FU Berlin.

**Table I.** Crystal Data and Experimental Conditions

formula	C <sub>3</sub> H <sub>3</sub> SF <sub>7</sub>
formula weight	204.11
space group <sup>a</sup>	P2 <sub>1</sub> /n (no. 14)
z	8
d (g/cm <sup>3</sup> )	2.113
V (nm <sup>3</sup> )	1.283
a (pm)	1709.0 (7)
b (pm)	647.8 (6)
c (pm)	1698.0 (7)
β (deg)	136.96 (6)
F(000)	800
θ (°C)	-151 (1)
abs. coeff (cm <sup>-1</sup> )	5.5
min. abs corr	1.232
max. abs corr	1.275
wave length (pm)	71.068
2θ range (deg)	4.0 < 2θ < 100.2
(h, k, l) <sub>min</sub>	-10, -13, -29
(h, k, l) <sub>max</sub>	29, 13, 21
scan width (deg)	1.44 + 0.26 tan θ
scan rate (deg min <sup>-1</sup> )	0.48-2.40
no. reflns collectd	10215
unobsd (I < 2σ(I))	1208
unique	7633

<sup>a</sup>By the transformation  $a' = 001$ ,  $b' = 010$ ,  $c' = -10-1$  a unit cell of space group P2<sub>1</sub>/c is obtained that has a monoclinic angle closer to 90°,  $a' = 1698$ ,  $b' = 647.8$ ,  $c' = 1249.8$  pm,  $\beta' = 111.05^\circ$ . All crystallographic calculations, however, were carried out in the P2<sub>1</sub>/n cell which was originally chosen by the diffractometer software.

41 °C, mp -105 °C; IR (gas) 2970 (w), 1734 (w), 1460 (vw), 1360 (vw), 1300 (s), 1215 (vw), 1169 (s), 1120 (m), 990 (m), 859 (s), 838 (s), 723 (m), 645 (w) cm<sup>-1</sup>; MS,  $m/z = 204$  (M<sup>+</sup>), 108 (SF<sub>4</sub><sup>+</sup>), 96 (C<sub>3</sub>F<sub>3</sub><sup>+</sup>), 95 (C<sub>3</sub>H<sub>2</sub>F<sub>3</sub><sup>+</sup>), 89 (SF<sub>3</sub><sup>+</sup>), and smaller fragments; <sup>1</sup>H NMR δ = 1.9 ppm, <sup>4</sup>J<sub>H-F</sub> = 9.29 (eq), -5.1, -2.9 (ax), 1.3 (CF) Hz; <sup>19</sup>F NMR a<sub>2</sub>b<sub>2</sub>c<sub>3</sub> spectrum, δ<sub>a</sub> 66.7, δ<sub>b</sub> 56.1, δ<sub>c</sub> 46.6, δ<sub>x</sub> -53.8 ppm; J<sub>ab</sub> = 159.1, J<sub>ac</sub> = 156.1, J<sub>bc</sub> 13.9, J<sub>ax</sub> 10.04, J<sub>bx</sub> -32.8; J<sub>cx</sub> -10.2 Hz. Anal Calcd for C<sub>3</sub>H<sub>3</sub>F<sub>7</sub>S: C, 17.64; H, 1.47; F, 65.19; S, 15.68. Found: C, 17.90; H, 1.48; F, 65.30; S, 15.57.

*cis*-ClF<sub>4</sub>SCH(CH<sub>3</sub>)CF<sub>3</sub>. F<sub>4</sub>S=C(CH<sub>3</sub>)CF<sub>3</sub> (1.6 g, 8 mmol) and gaseous HCl (0.3 g, 8 mmol) are condensed into an 100-mL stainless steel autoclave and kept there for 12 h under stirring. Fractional condensation in vacuo through -100 °C and -196 °C cold traps yields 0.8 g (42%) of the product in the -100 °C trap as a colorless liquid: bp 87 °C; IR (gas) 2996 (w), 1487 (m), 1393 (m), 1264 (s), 1198 (s), 1132 (m), 1062 (m), 834 (m), 677 (m), 620 (m) cm<sup>-1</sup>; MS,  $m/z = 221$  (M<sup>+</sup> - F), 205 (M<sup>+</sup> - Cl), 143 (SF<sub>4</sub>Cl<sup>+</sup>), 97 (C<sub>3</sub>H<sub>4</sub>F<sub>3</sub><sup>+</sup>), and smaller fragments; <sup>1</sup>H NMR δ = 4.83, 2.10 ppm, J<sub>H-H</sub> = 6 Hz; <sup>19</sup>F NMR abcdx<sub>3</sub> spectrum, δ<sub>a</sub> = 154.90, δ<sub>b</sub> = 111.43, δ<sub>c</sub> = 57.02, δ<sub>d</sub> = 94.33, δ<sub>x</sub> = -68.91 ppm; J<sub>ab</sub> = 151, J<sub>ad</sub> = 151, J<sub>bc</sub> = 86, J<sub>cd</sub> = 86, J<sub>bx</sub> = 18, J<sub>cx</sub> = 18, J<sub>dx</sub> = 8, J<sub>b-H</sub> = 9, J<sub>c-H</sub> = 9 Hz.

**X-ray Measurement.** The compound F<sub>4</sub>S=C(CH<sub>3</sub>)CF<sub>3</sub> is a stable, volatile liquid; crystals had to be grown below -105 °C. A glass tube of 0.5-mm diameter, 0.01-mm wall thickness, and 25-mm length was filled with a 3-mm liquid column at one end by distillation in vacuo and closed at the opposite end, too. The sample was mounted on a single-crystal diffractometer with a special arcless head, and there it was cooled down until solidification occurred at -125 °C. A single crystal was obtained by setting the temperature to a few degrees below the melting point, melting the greater part of the sample from the lower side of the column with a coaxial coil of heating wire, then very slowly moving the phase border face in the opposite, downward direction with an electronic control device for the heat output of the coil, and finally annealing at the present temperature.<sup>19</sup> The crystal was slowly cooled down to -151 (1) °C. The cooling was done with an N<sub>2</sub> gas stream device<sup>20</sup> that was combined with the computer-controlled SIEMENS four-circle diffractometer. Zr-filtered Mo Kα radiation was used. Cell constants and orientation matrix were obtained by least-squares refinement of 20 automatically centered reflections with 27° < 2θ < 44°. This determination was repeated whenever the intensity of any one of seven standard reflections, which were measured every 60 min, dropped by more than 3%.

Further experimental details are given in Table I.

For 2θ < 60° all reflections of a hemisphere and for 60° < 2θ < 75° all reflections of a quadrant were measured, and in the upper range 75°

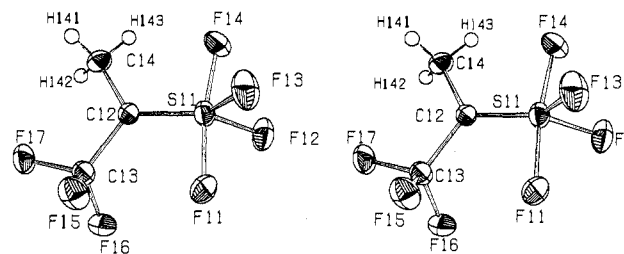


**Figure 1.** ORTEP stereo drawing of (2,2,2-trifluoro-2-methyl-ethylidene)sulfur tetrafluoride, molecule 1.

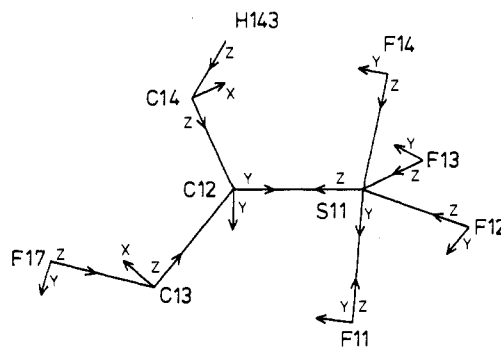


**Figure 2.** The definitions of site coordinate systems used in the multipole refinement.

≤ 2θ ≤ 100.2° only 1362 strong reflections from a quadrant were measured. The intensities were corrected for the changing crystal volume hit by the X-ray beam.<sup>21</sup> The internal R value for merging 5053 reflections down to 2472 reflections was 0.016.

**Structure Refinements.** The structure was solved with the direct methods program SHELXS.<sup>22</sup> Full-matrix least-squares refinements and related calculations were carried out with the X-TAL system<sup>23</sup> of crystallographic computer programs. A 1/σ(F<sub>o</sub>) weight scheme was used to refine one scale factor, positional parameters, anisotropic and isotropic thermal parameters for the non-hydrogen and hydrogen atoms, and an isotropic extinction coefficient. The atomic scattering factors used are from references 24 and 25. The anomalous dispersion was corrected for by using the values from *The International Tables of Crystallography*.<sup>26</sup> Except for the hydrogen atomic parameters and the isotropic extinction parameter, all parameters were refined with the high-order data with (sin θ)/λ > 0.007 nm<sup>-1</sup>. The number of unique low-order reflections was 3680, of which 230 had an intensity < 4σ(I). The refinement of the above stated parameters on these had an R value of 0.036. The strongest F<sub>c</sub> correction by isotropic extinction was 0.89 for the reflection -4 0 4.

**Multipole Refinement.** The aspherical atomic electron density ρ(r) is described in terms of spherical harmonics<sup>27</sup>

$$\rho(r) = \rho_c(r) + P_v \rho_v(r) + \sum_{l=0}^4 R_l(k'r) \sum_{m=-l}^l i^m y_{lm}(r/r)$$

where ρ<sub>c</sub> and ρ<sub>v</sub> are the spherical Hartree-Fock core and valence densities, R<sub>l</sub> and y<sub>lm</sub> stand for the Slater-type radial and real normalized angular functions, respectively. The P<sub>v</sub>, ρ<sub>v</sub>, R<sub>l</sub> and κ, κ' expansion-contraction factors are refinable variables in addition to the conventional crystallographic parameters. The Fourier-Bessel transforms (J<sub>o</sub>) of ρ<sub>c</sub> and ρ<sub>v</sub> are given in ref 28, and the parameters for the Slater

(21) Luger, P. KAPCOR, a capillary volume correction program; Freie Universität Berlin, 1984; unpublished.

(22) Sheldrick, G. M. SHELXS-86, Program for Crystal Structure Solution; University of Goettingen, Germany, 1986.

(23) Hall, S. R.; Stewart, J. M.; Eds. XTAL 2.2. *Users Manual*; University of Western Australia, Nedlands, WA and University of Maryland, College Park, MD, 1987.

(24) Cromer, D. T.; Mann, J. B. *Acta Crystallogr., Sect. A* **1968**, *A24*, 321.

(25) Stewart, R. F.; Davidson, E. R.; Simpson, W. T. *J. Chem. Phys.* **1965**, *42*, 3175.

(26) *International Tables for X-ray Crystallography IV*; Ibers, J. A., Hamilton, W. C., Eds.; The Kynoch Press: Birmingham, England, 1974; p 148.

(27) Hansen, N. K.; Coppens, P. *Acta Crystallogr.* **1978**, *A34*, 909.

(28) Reference 26, pp 102-147.

(19) Luger, P.; Buschmann, J. *J. Am. Chem. Soc.* **1984**, *106*, 7118.

(20) Dietrich, H.; Dierks, H. *Messtechnik (Braunschweig)* **1970**, *78*, 184.

Table II. Summary of Refinements

	spherical atom	spherical atom high order	multipole
$w$	$1/\sigma( F_o )$	$1/\sigma( F_o )$	$1/\sigma( F_o )$
(sin $\theta$ )/ $\lambda$ range ( $\text{pm}^{-1}$ )	0.000–0.0108	0.007–0.0108	0.000–0.0108
no. of unique obsd reflcn $m$	6628	3178	6178 ( $I > 4\sigma(I)$ )
no. of variables $n$	223	199	272
$R = \sum( F_o  -  F_c ) / \sum  F_o $	0.041	0.054	0.029
$R_w = [\sum w( F_o  -  F_c )^2 / \sum w  F_o ^2]^{1/2}$	0.029	0.039	0.019
$S = [\sum w( F_o  -  F_c )^2 / (m - n)]^{1/2}$	3.84 (3)	1.24 (2)	

Table III. Atomic Parameters of F<sub>4</sub>S=C(CH<sub>3</sub>)CF<sub>3</sub> (UEQ and  $U$  in nm<sup>2</sup>)

atom	$x$	$y$	$z$	UEQ, $U$
S11	0.58618 (1)	0.00088 (3)	0.20198 (2)	3.007 (2)
F11	0.56247 (4)	-0.2413 (2)	0.18844 (4)	4.562 (8)
F12	0.69393 (7)	-0.05280 (9)	0.22967 (4)	4.769 (7)
F13	0.64285 (5)	-0.02157 (9)	0.32724 (8)	4.991 (8)
F14	0.63113 (5)	0.2323 (2)	0.23474 (5)	4.831 (7)
F15	0.35314 (4)	-0.2156 (1)	0.06675 (5)	4.762 (6)
F16	0.38661 (4)	-0.2443 (1)	-0.03313 (5)	4.507 (6)
F17	0.26639 (6)	-0.0198 (1)	-0.07915 (6)	4.022 (6)
C12	0.45799 (7)	0.0602 (1)	0.08291 (7)	2.676 (7)
C13	0.36786 (8)	-0.1065 (1)	0.01129 (8)	3.150 (8)
C14	0.4197 (1)	0.2777 (1)	0.0359 (1)	3.88 (1)
S21	0.98099 (2)	-0.00718 (3)	0.12762 (2)	3.327 (2)
F21	0.95354 (5)	-0.2482 (2)	0.10143 (4)	4.997 (8)
F22	1.10860 (8)	-0.06385 (9)	0.20055 (6)	4.762 (7)
F23	0.98734 (4)	-0.03969 (9)	0.22393 (7)	5.677 (8)
F24	1.02520 (5)	2.2214 (2)	0.17547 (5)	5.132 (8)
F25	0.74079 (5)	-0.2055 (1)	-0.08101 (4)	5.390 (7)
F26	0.84501 (5)	-0.2381 (1)	-0.10856 (4)	4.709 (6)
F27	0.71544 (6)	-0.0055 (1)	-0.19880 (7)	4.735 (6)
C22	0.87827 (7)	0.0628 (1)	-0.00453 (8)	3.138 (8)
C23	0.79697 (6)	-0.0986 (1)	-0.09574 (7)	3.629 (7)
C24	0.85743 (8)	0.2853 (1)	-0.04152 (8)	4.572 (9)
H141	0.365 (2)	0.335 (3)	0.034 (2)	4.3 (3)
H142	0.379 (1)	0.280 (2)	-0.043 (1)	5.2 (3)
H143	0.485 (1)	0.372 (2)	0.075 (1)	5.9 (3)
H241	0.8295 (9)	0.367 (2)	-0.0186 (9)	5.3 (3)
H242	0.805 (1)	0.287 (2)	-0.127 (1)	7.2 (3)
H243	0.926 (1)	0.348 (2)	-0.0129 (9)	5.6 (3)

orbitals were taken from ref 27. For the hydrogen atoms the same scattering factor table was used as in the conventional refinement. Equivalent atoms for the two crystallographically independent molecules were constrained to have the same valence deformation density. This constraint was supported by the same geometrical parameters of the two molecules obtained after conventional high-order refinement: the mean interatomic distances and bond angles, averaged over the equivalent bonds, yield significantly equal values. Also similar features are exhibited by the X–X deformation densities. An increase for the significance in modelling the EDD could be expected by taking advantage of the observed congruence between the two molecules. To reduce the number of parameters to be refined as far as possible the multipole populations for the chemically equivalent atoms were constrained to be equal. This restraint yields one S and one H atom and three different C(C12, C13, C14) and F(F11, F12, F15) atoms, for which the valence asphericity was described independently. The local atomic coordinate systems as defined for these atoms are illustrated in Figure 2. In the given local frame, mm2, m, and 3m site symmetry was assumed for S, C12, and for both C13 and C14, respectively. To keep the cylindrical symmetry of the X–F and C–H bonds, no density asphericity perpendicular to the bonds was allowed to contribute to the scattering of F and H atoms ( $P_{lm} = 0$  for  $m \neq 0$ ).

The non-hydrogen atoms were treated up to the hexadecapolar level in the multipole expansion. For the H atoms the thermal parameters were fixed, and the density deformation was represented by a dipole along the bond. When the radial shielding ( $\kappa, \kappa'$ ) parameters were included in the refinement, the atomic charges slowly converged to more or less unrealistic values. At the same time the estimated standard deviations of the multipole populations and thermal parameters increased. As, in addition, the obtained vibrational tensors violated the rigid bond postu-

Table IV. Multipole Populations of F<sub>4</sub>S=C(CH<sub>3</sub>)CF<sub>3</sub>

$l$	$m$	S11	F11	F12	F15	C12	C13	C14	H141
0	0	5.18	7.19	7.09	7.09	4.09	4.11	3.96	0.95
1	1					0.12			
1	-1				-0.04				
1	0	0.11	0.14	0.22	0.05		0.07	0.01	0.20
2	0	0.14	0.15	0.08	-0.11	-0.14	0.12	-0.02	
2	2	-0.03				-0.01			
2	-2					0.03			
3	0	0.30	0.09	0.01	0.02			0.35	0.38
3	1					0.05			
3	-1					-0.03			
3	2	-0.09							
3	3					0.24	0.26	-0.17	
3	-3					0.02			
4	0	0.00	0.09	0.01	-0.01	0.01	0.07	0.11	
4	2	0.30				0.03			
4	-2					0.04			
4	3						-0.03	0.14	
4	4	0.07				0.04			
4	-4					0.06			

Table V. Bond Lengths (pm), Selected Valence Angles (deg), and Selected Dihedral Angles (deg) of F<sub>4</sub>S=C(CH<sub>3</sub>)CF<sub>3</sub><sup>a</sup>

a. Bond Lengths			
S11–F11	159.3 (2)	S11–F12	156.9 (4)
S11–F13	157.0 (5)	S11–F14	158.6 (2)
S11–C12	159.9 (3)	F15–C13	134.0 (3)
F15–C13	134.9 (3)	F17–C13	133.7 (3)
C12–C13	150.9 (3)	C12–C14	151.2 (2)
S21–F21	159.6 (2)	S21–F22	157.1 (4)
S21–F23	156.9 (4)	S21–F24	158.8 (2)
S21–C22	160.0 (4)	F25–C23	134.7 (3)
F26–C23	134.1 (3)	F27–C23	134.3 (3)
C22–C23	150.8 (2)	C22–C24	150.7 (3)
b. Selected Valence Angles (deg)			
F11–S11–F14	170.40 (5)	F21–S21–F24	170.50 (5)
F11–S11–F12	94.9 (1)	F21–S21–C22	95.1 (1)
F12–S11–F13	98.4 (2)	F22–S21–F23	98.5 (2)
F12–S11–C12	130.9 (2)	F22–S21–C22	129.7 (2)
F13–S11–C12	130.7 (2)	F23–S21–C22	131.8 (2)
F14–S11–C12	94.7 (1)	F24–S21–C22	94.4 (2)
S11–C12–C13	119.6 (2)	S21–C22–C23	119.1 (2)
S11–C12–C14	123.7 (1)	S21–C22–C24	122.6 (1)
C13–C12–C14	116.6 (2)	C23–C22–C24	118.3 (2)
F15–C13–C12	114.6 (2)	F25–C23–C22	114.4 (3)
F16–C13–C12	113.9 (2)	F26–C23–C22	114.8 (3)
F17–C13–C12	109.2 (2)	F27–C23–C22	109.1 (2)
c. Selected Dihedral Angles (deg)			
F11–S11–C12–C13	3.7 (2)	F21–S21–C22–C23	3.4 (2)
F11–S11–C12–C14	-176.5 (2)	F21–S21–C22–C24	-178.3 (2)
F12–S11–C12–C13	93.6 (2)	F22–S21–C22–C23	93.6 (2)
F12–S11–C12–C14	-86.5 (2)	F22–S21–C22–C24	-88.0 (2)
F13–S11–C12–C13	-86.4 (2)	F23–S21–C22–C23	-86.7 (2)
F13–S11–C12–C14	93.5 (2)	F23–S21–C22–C24	91.7 (2)
F14–S11–C12–C13	-176.7 (2)	F24–S21–C22–C23	-176.6 (2)
F14–S11–C12–C14	3.2 (2)	F24–S21–C22–C24	1.7 (2)

<sup>a</sup> Estimated standard deviations are in parentheses.

late,<sup>29</sup> the  $\kappa$  values were fixed to 1.0 for all atoms.

In comparison to the spherical atom model, multipole refinement gave improved agreement (Table II) with reduced estimated standard deviations for the atomic parameters (Table III). Significantly longer bond distances were obtained, especially for S–F and C–F bonds. The final multipole populations and geometrical parameters are listed in Tables IV and Va–c.

## Results

The alkylidenesulfur tetrafluoride F<sub>4</sub>S=C(CH<sub>3</sub>)CF<sub>3</sub> was prepared by elimination of "BrF" from F<sub>5</sub>CBr(CH<sub>3</sub>)CF<sub>3</sub> with *n*-C<sub>4</sub>H<sub>9</sub>Li at low temperature. The yield of this reaction is low as a parallel elimination renders the isomer F<sub>5</sub>SC(CH<sub>3</sub>)=CF<sub>2</sub>, so that purification by gas chromatography is necessary.

The reaction of  $F_4S=C(CH_3)CF_3$  with HCl leads to *cis*- $CISF_4CH(CH_3)CF_3$ . No trace of the *trans* isomer is observed by NMR spectroscopy. This cannot be the result of inherent instabilities of such *trans* systems, since *trans*- $CISF_4R$  compounds were already prepared a long time ago and found to be stable.<sup>30</sup> Without stringent proof it can thus be assumed that a *cis* addition is the result of a four-membered ring intermediate state. The addition direction is also selective; there is no *cis*- $HSF_4CCl-(CH_3)CF_3$ . This may be the result of a small polarity of the  $C=S$  bond in terms of an ylidic model. Even more likely, such a species may not be stable, so that only one of the two regioisomers is observed. The resulting *cis*- $CISF_4CH(CH_3)CF_3$  molecule shows all F atoms on sulfur being chemically and magnetically non-equivalent due to the dissymmetric carbon atom.

The general molecular shape of  $F_4S=C(CH_3)CF_3$  may be derived from a trigonal bipyramid around sulfur. This is obvious from the NMR spectra, since the (S)F signals give rise to an  $a_2bc$  spectrum. This means that the two carbon substituents should lie in plane with the two axial fluorine atoms on sulfur, as predicted by straightforward molecular models.<sup>31</sup> The X-ray investigation proves this to be correct, see Figure 1 and Table Va-c: Both crystallographically independent molecules have the same structure. Since there are no geometrical constraints by symmetry on either molecule, small deviations from the ideal structure, most likely caused by steric interaction of the large  $CF_3$  group, can be determined. The environment around the double-bonded carbon atom is planar in both molecules. The same holds for the sulfur environment, if the equatorial fluorine atoms are excluded. Both planes have a small angle of  $3.9^\circ$  (molecule I) and  $3.0^\circ$  (molecule II) with each other. This dihedral deviation from general planarity is considered small. So, for example, a few unsymmetrically substituted stilbene derivatives are reported, where such a deviation from planarity reaches angles of up to  $10^\circ$ .<sup>32</sup>

**Charge Density Analysis.** The electron density deformations due to chemical bonds can be demonstrated by subtracting the density of the promolecule from the total molecular charge distribution. The promolecular density is the superposed density of the undisturbed, spherically averaged atoms (spherical atom model, SAM) placed at the positions which are determined by the least-squares refinement. This visualization of the electron migration is the most widely used procedure, although it has arbitrariness in the choice of the proper atomic ground state to be subtracted.<sup>33,34</sup>

An alternative promolecule can be built of superposing the charge densities calculated for oriented atomic ground states or chemically expected hybridization<sup>35</sup> (oriented atom model, OAM). This method turned out to have special importance in illustrating charge localization along bonds to atoms which have nearly closed valence shells.<sup>36</sup>

To map the experimentally determined EDD it is common procedure to evaluate the difference of the molecular and promolecular densities directly from the observed and calculated structure factors. This means to calculate the following Fourier series (X-X synthesis)

$$\Delta\rho(\mathbf{r}) = \sum_{\mathbf{H}} (F_o(\mathbf{H}) - F_c(\mathbf{H})) \exp(-2\pi i\mathbf{H}\mathbf{r})$$

where  $F_o$  and  $F_c$  are the observed and calculated structure factors. The  $F_c$ 's are usually calculated from the positional and thermal atomic parameters of a spherical refinement with high-order reflections observed at high scattering angles. In case of the full

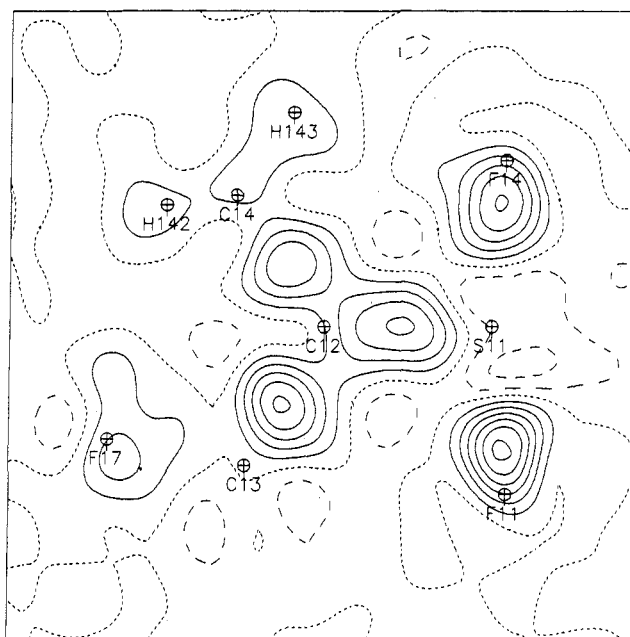
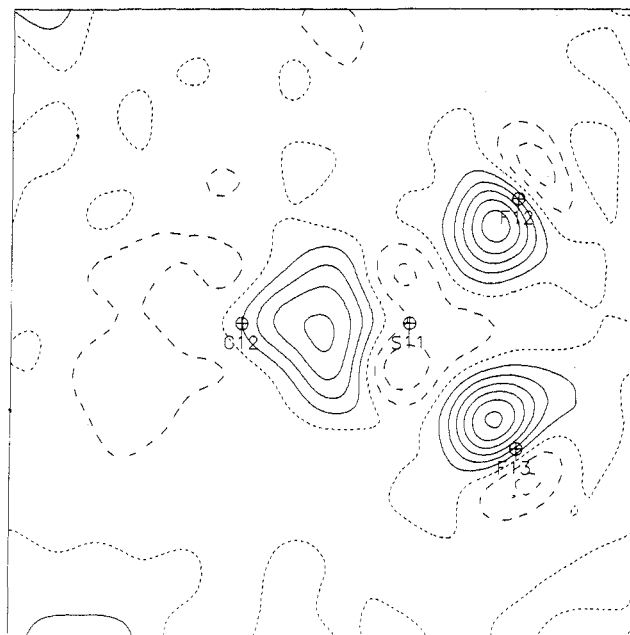


Figure 3. Averaged dynamic deformation density (DDD): (a) equatorial plane and (b) axial plane. The contour intervals are  $100 \text{ e}/\text{nm}^3$ , and the standard deviation is estimated to be  $50 \text{ e}/\text{nm}^3$  in a general position.

data set multipole refinement, the phases of  $F_o$ 's are obtained from the parameters of the fitted aspherical model; this procedure constitutes DDD. To reduce the experimental noise in the density maps only the low-order data ( $(\sin \theta)/\lambda < 0.0075 \text{ \AA}^{-1}$ ) with  $F > 4\sigma(F)$  were included in the Fourier summation.<sup>37,38</sup> Eliminating the temperature factors yields the static deformation density SDD again with reference to both SAM and OAM promolecules; for this, the experimental and model density are directly calculated, not by Fourier transformation, and subtracted. The SDD can be considered as a model of the observed density extrapolated to zero atomic vibration.

The DDD in the equatorial and axial planes, calculated as the averaged densities of the two independent molecules, are displayed in Figure 3a,b. They exhibit well-defined excess density in the C-C bonds. The anisotropy observed between the sulfur and the carbon atom can clearly be attributed to a double bond.

Peaks along the S-F bond paths are localized close to the more electronegative F ligands. No excess density can be found either

(30) Yu, S. L.; Shreeve, J. M. *Inorg. Chem.* **1976**, *15*, 14. Kitasume, T.; Shreeve, J. M.; *J. Chem. Soc., Chem. Commun.* **1976**, 982.

(31) Thrasher, J. *Inorg. Chem.* In press.

(32) Cantrell, T. S.; Silvertown, J. V. *J. Org. Chem.* **1979**, *44*, 4477. Ruban, G.; Zobel, P.; Kossmehl, G.; Nuck, R. *Chem. Ber.* **1980**, *113*, 3384. See, also: Roberts, P. J.; Kennard, O. *Cryst. Struct. Commun.* **1973**, *2*, 153.

(33) Dunitz, J. D.; Schweizer, W. B.; Seiler, P. *Helv. Chim. Acta* **1983**, *66*, 123.

(34) Seiler, P.; Schweizer, W. B.; Dunitz, J. D. *Acta Crystallogr.* **1984**, *B40*, 319.

(35) Schwarz, W. H. E.; Valtazanos, P.; Ruedenberg, K. *Theor. Chim. Acta* **1985**, *68*, 471.

(36) Takazawa, H.; Ohba, S.; Saito, Y. *Acta Crystallogr.* **1989**, *B45*, 432.

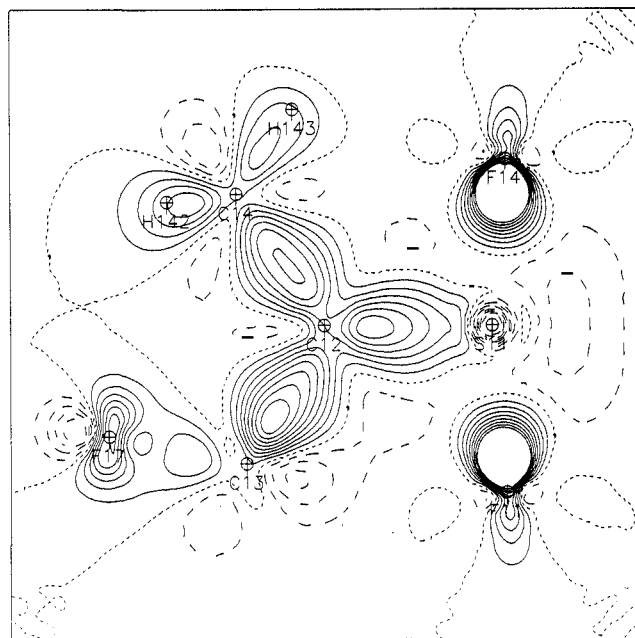
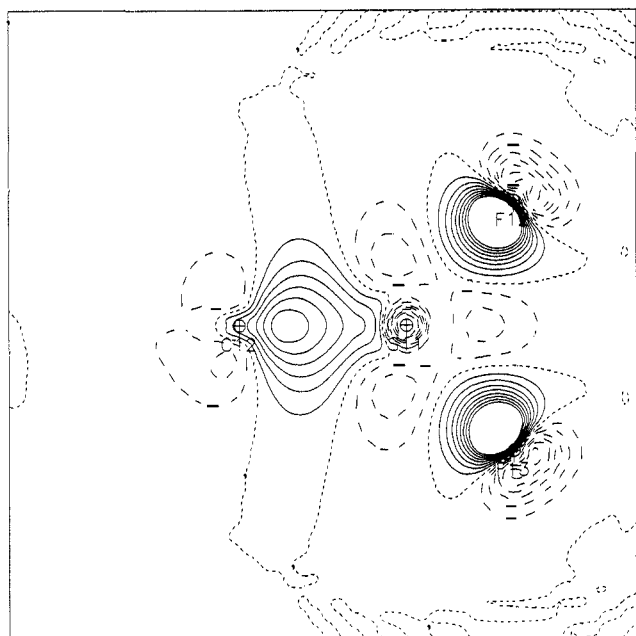


Figure 4. Static model deformation density (SDD) calculated from the refined multipole populations with respect to SAM: (a) equatorial plane and (b) axial plane. Qualitatively unpolar C-C and C-H bonds can be distinguished from semipolar C-C and C-S bonds and polar C-F and S-F bonds.

in the C-F bonds or in the lone-pair region of the fluorine atoms, which is in good agreement with previous observations.<sup>33,34</sup> Planes of the SDD calculated with respect to SAM, as shown in Figures 4-6, give a "noise-free" representation of the observed densities. Peaks around the carbon atoms are sharper than and topologically similar to those of the DDD.

The deformation around the fluorine atoms exhibits a strange appearance that needs to be commented on. A typical situation occurs for the fluorine atoms bonded to the carbon atom. A negative area and charge accumulation appear in the bond and the perpendicular direction, respectively (Figure 6a). A similar quadrupolar pattern was found in the theoretical EDD maps for the F<sub>2</sub> molecule, and it was attributed to the use of SAM for constructing the promolecule.<sup>35</sup> When spherical atoms are used as the basis for a simple comparison, more than two electrons are assumed in the bond, i.e., the free F atom density is obtained from the  $2p_{\sigma}^{5/3}$ ,  $p_{\pi}^{10/3}$  state. An obvious alternative reference density

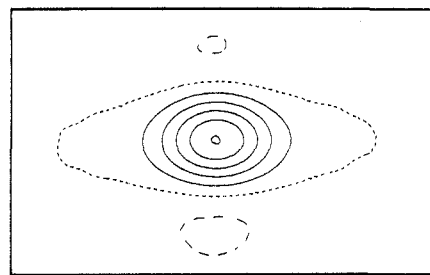


Figure 5. SDD in the plane perpendicular to the C-S double bond, same distance from both atoms. The double bond nature is clearly visible.

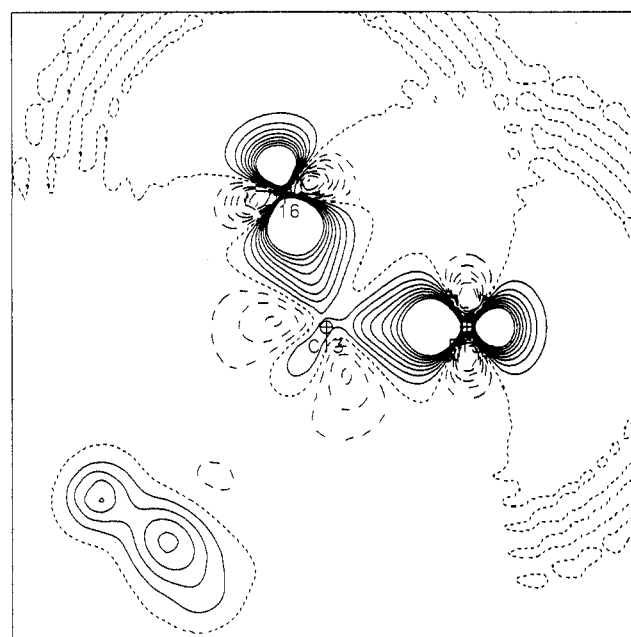
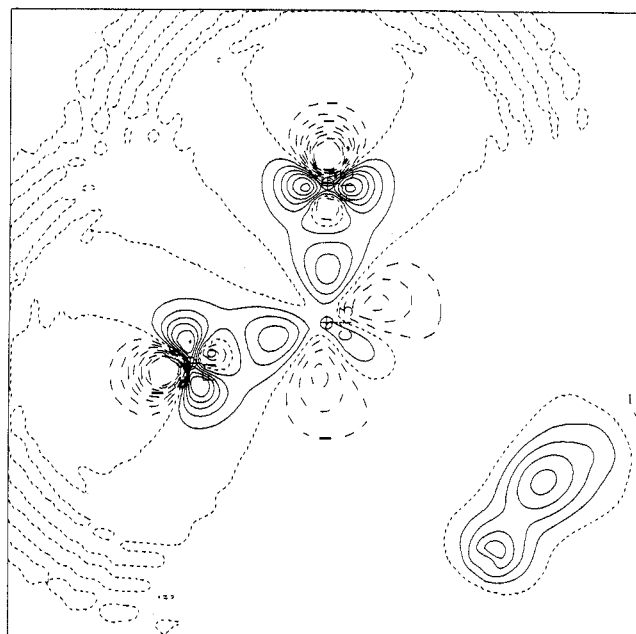


Figure 6. SDD in the C13-F15-F16 plane: (a) reference atomic density from SAM and (b) reference density from OAM.

for F can be composed by putting only one electron on a  $2p_{\sigma}$  orbital oriented toward the carbon atom ( $2p_{\sigma}^1$ ,  $2p_{\pi}^4$  state).

The SDD with respect to this OAM for F, as shown in Figure 6b, reveals the picture that one would expect on the basis of simple MO formalism for a covalent bond, i.e., charge buildup between the atoms at the expense of charge in the nonbonded regions. For

representing the valence deformation around the F atoms attached to the sulfur atom, the subtraction of the oriented reference density yields similar local results, but the bonds remain depleted of charge.

All attempts failed to make bond peaks visible midway between the S-F atoms by creating properly oriented reference densities for S. The trigonal-bipyramidal arrangement of the sulfur atom can be described by  $sp^2$ ,  $d_{xz}$ ,  $p_z$ , and  $d_{y^2}$  hybridization for the equatorial  $\sigma$  and  $\pi$ , and the axial  $\sigma$  orbitals, respectively. After subtracting the aspherical density calculated from these assumed hybrid orbitals, the charge-depleted region seemed to be unaffected. The reason for this failure must be the loss of net charge at the sulfur that cannot be compensated by a neutral reference density even if it should be properly oriented.

### Conclusion

The accurate single-crystal X-ray diffraction measurement on  $F_4S=C(CH_3)CF_3$  proves that both parts of the molecule, the  $S=CC_2$  and the  $F_3S=C$  part, are flat. These so defined planes have a dihedral angle of only 3-4°. This molecule therefore does not undergo nonclassical distortions, as does its triple-bonded relative,  $F_3S=CCF_3$ .<sup>39</sup>

The electron deformation density of  $F_4S=C(CH_3)CF_3$  exhibits detailed features of the bonding, especially if the oriented atom model (OAM) is used for the promolecule. The difficulty of this method, if applied to atoms with a higher valence state, is that no trivial oriented reference density can be established, as is the case for atoms of low valence state. It must be realized that the preconception used in the interpretation of charge redistribution will influence the results.<sup>33</sup>

**Acknowledgment.** This work has been supported by the Deutsche Forschungsgemeinschaft and the Fonds der Chemischen Industrie.

**Supplementary Material Available:** Listings of atomic parameters and least-squares planes (7 pages); listings of observed and calculated structure factors (65 pages). Ordering information is given on any current masthead page.

(37) Wang, Y.; Blessing, R. H.; Ross, F. K.; Coppens, P. *Acta Crystallogr.* **1976**, *B32*, 572.

(38) Denne, W. A. *Acta Crystallogr.* **1977**, *A33*, 438.

(39) Seppelt, K. *Angew. Chem.* In press; *Angew. Chem., Int. Ed. Engl.* In press.

## Mechanism of Reaction of Hydroxide Ion with Dinitrochlorobenzenes

Radu Bacaloglu,<sup>1a</sup> Andrei Blaskó, Clifford Bunton,\* Ellen Dorwin, Francisco Ortega,<sup>1b</sup> and César Zucco<sup>1c</sup>

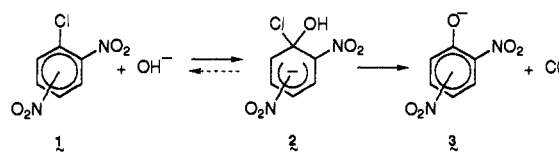
Contribution from the Department of Chemistry, University of California, Santa Barbara, California 93106. Received June 11, 1990

**Abstract:** Formation of dinitrophenoxide ion from 2,4- and 2,6-dinitrochlorobenzene (2,4- and 2,6-DNCB) and  $OH^-$  ( $OD^-$ ) in 70:30 and 80:20 (v/v) DMSO- $H_2O$  ( $D_2O$ ) is accompanied by extensive  $^1H$  NMR line broadening of unreacted substrate and exchange of arene hydrogen with  $D_2O$ , which is quantitative at the 3-position of 2,4-DNCB. Unproductive Meisenheimer complexes are detected spectrophotometrically in the course of reaction. For reaction of 2,4-DNCB, the Meisenheimer 3-complex is formed first and then the more stable 5-complex can be detected and characterized by NMR spectrometry. There is no hydrogen exchange of Meisenheimer complexes or dinitrophenoxide ions and their  $^1H$  NMR signals are not broadened. These results do not fit the classical mechanism of single-step nucleophilic addition, but they, and the kinetic results, are fitted by a reaction scheme involving single-electron transfer from  $OH^-$  to give a charge-transfer complex of  $OH^-$  and a radical anion which collapses to give Meisenheimer complexes and aryl oxide ion. This scheme is consistent with MO calculations by the AM1 method.

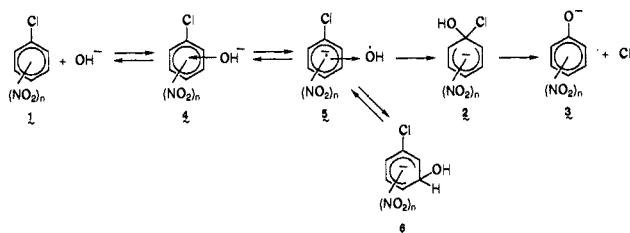
The mechanism of aromatic nucleophilic substitution of dinitrochlorobenzenes (**1**), for example, in polar, hydroxylic, solvents has been assumed to involve rate-limiting formation of a  $\sigma$  or Meisenheimer complex (**2**), as in Scheme I for reaction of  $OH^-$  with 2,4- or 2,6-dinitrochlorobenzene (2,4- and 2,6-DNCB).<sup>2</sup> Loss of  $Cl^-$  from **2** should be fast in polar solvents. Unproductive Meisenheimer complexes form in the course of some reactions.

Anion radicals are intermediates in aromatic nucleophilic substitutions in apolar solvents<sup>3</sup> and radical chain reactions have

Scheme I



Scheme II



(1) Present address: (a) Department of Chemistry, Rutgers SUNJ, Piscataway, NJ 08855. (b) Department of Physical Chemistry, Facultad de Ciencias Químicas, Universidad Complutense, 28040 Madrid, Spain. (c) Departamento de Química, Federal University of Santa Catarina, 88049 Florianópolis, SC, Brasil.

(2) (a) Bunnett, J. F. *Q. Rev., Chem. Soc.* **1958**, *12*, 1. (b) Sauer, J.; Huisgen, R. *Angew. Chem.* **1960**, *72*, 294. (c) Buncl, E.; Norris, A. R.; Russell, K. E. *Q. Rev., Chem. Soc.* **1968**, *22*, 123. (d) Miller, J. *Aromatic Nucleophilic Substitution*; Elsevier: New York, 1968. (e) Bernasconi, C. F. *Chimia* **1980**, *34*, 1.

(3) (a) Russell, G. A.; Janzen, G. E. *J. Am. Chem. Soc.* **1962**, *84*, 4153. (b) Shein, S. M.; Brykovevskaya, L. V.; Pishchugin, F. V.; Starichenko, V. F.; Panfilov, V. N.; Voevodski, V. V. *Zh. Strukt. Khim.* **1970**, *11*, 243. (c) Blumenfeld, L. A.; Brykovevskaya, L. V.; Formin, G. V.; Shein, S. M. *Zh. Fiz. Khim.* **1970**, *44*, 931. (d) Ivanova, T. M.; Shein, S. M. *Zh. Org. Khim.* **1986**, *16*, 1221. (e) Abe, T.; Ikegami, Y. *Bull. Chem. Soc. Jpn.* **1976**, *49*, 3227; **1978**, *51*, 5, 196. (f) Mariani, C.; Modena, G.; Pizzo, G. P.; Scorrano, G.; Kistenbruggler, L. *J. Chem. Soc., Perkin Trans. 2* **1979**, 1187.

also been identified,<sup>4</sup> in contrast to the behavior in polar, hydroxylic, solvents. However, recent kinetic and NMR spectroscopic evidence suggests that reaction occurs by electron transfer from the nucleophile into the antibonding orbital of the aromatic

(4) Bunnett, J. F. *Acc. Chem. Res.* **1978**, *11*, 413.